Visualisation of the structure transfer between an oriented polymer melt and the semi-crystalline state

Norbert Stribeck[a]*, Rüdiger Bayer[b], Peter Bösecke[c], Armando Almendarez Camarillo[a]

[a] Institut für Technische und Makromolekulare Chemie, Universität Hamburg, Bundesstrasse 45, 20146 Hamburg, Germany

[b] Institut für Werkstofftechnik, Universität GH Kassel, Mönchebergstrasse 3, 34125 Kassel, Germany

[c] ESRF, 6 rue Jules Horowitz, B.P. 220, 38043 Grenoble Cedex 9, France

submitted to *Polymer* 09.07.2004

Abstract

Nanostructure evolution of highly oriented polyethylene during cautious melting and crystallisation is investigated with high time resolution by means of small–angle X–ray scattering (SAXS) and wide–angle X–ray scattering (WAXS). The two-dimensional SAXS patterns are transformed to the multidimensional chord distribution function (CDF) in physical space. The results are continuous smooth movies of the structure evolution which elucidate the mechanisms of structure evolution.

We find that crystallisation is preceeded by a peculiar nanostructure which we associate to the network of the entangled chains in the melt. This structure holds the key for the understanding of crystallite arrangement. The next stages of structure evolution are a fast lateral growth of lamellae from nuclei located at the ends of the entangled strands towards regions with lower entanglement density; thickness growth away from the entanglement strands accompanied by increase of perfection within the layers; and, finally, the crowding of the remnant amorphous phase by swarms of secondary crystalline blocks that form short-range networks both with the primary lamellae and with each other.

Keywords: Polymer Physics; Polymer Engineering;

1 Introduction

The understanding of polymer crystallisation is central for the tailoring of materials properties and again is in the scientific discussion [1–7]. As the result of crystallisation a nanostructure comprising crystalline domains in an amorphous matrix is formed. We visualise this process from two-dimensional (2D) X-ray scattering data collected *in situ* at the European Synchrotron Radiation Facility (ESRF) with high frequency. Data are transformed to physical space, yielding smooth movies of the structure evolution. In our experiments polyethylene with uni-

* Corresponding author. Tel.:+49-40-42838-3615; fax: +49-40-42838-6008. *E-mail address:* Norbert.Stribeck@desy.de

axial orientation is cautiously molten in order not to erase the orientation memory of the melt, then quenched to the crystallisation temperature. The nanostructure is presented as the multidimensional chord distribution function (CDF) [8, 9]. By application of this method to series of snapshots recorded with high frequency we obtain quasi-continuous movies in which structure formation mechanisms and their interrelationships are revealed. Comparison with earlier experiments [10–12] carried out at a rate of 30 snapshots per hour demonstrates that the quasi-continuous stream of high-quality multidimensional scattering data is required, if the mechanisms of crystallisation shall be studied. An essential condition for the experienced quantum leap with respect to the visualisation of nanostructure evolution is the availability of advanced 2D detectors, dynamic control of exposure time for each snapshot, and a brilliant synchrotron radiation source.

2 Experimental section

2.1 Material and setup

High-pressure injection moulded [9] rods from Lupolen 6021 D (BASF) are molten and crystallised in the synchrotron beam of beam line ID02 at the ESRF in Grenoble. Data are recorded using two 2D detectors (one detector for the collection of ultra small-angle X-ray scattering patterns in a distance of 10 m to the sample, and a second offset wide-angle X-ray scattering detector close to the sample). In the critical regions of the temperature profile the cycle time between consecutive snapshots is set to 7 s.

2.2 Data analysis

Data analysis is carried out with computer programs developed under Linux and pv-wave [13]. The computation of the CDF [8] is carried out automatically using an algorithm which resembles part of the back projection procedure used in medical computer tomography. Spot testing of individual snapshots from the large series turned out to be error-prone. Thus perception was improved by combining four patterns (small-angle X-ray scattering (SAXS), wide-angle X-ray scattering (WAXS) and the CDF from two different view points) in one picture frame and, finally, by collecting the series of frames in a movie. For this purpose the free programs PoVRay, ImageMagick, transcode and mplayer are utilised. In the running movie the mechanisms of nanostructure evolution become clear, and we can pick representative frames for the purpose of demonstration and an aspired quantitative analysis.

2.3 The CDF

The multidimensional chord distribution function (CDF) with fibre symmetry in real space, $z\left(r_{12}, r_3\right)$, can be computed from the fibre-symmetric SAXS pattern, $I\left(s_{12}, s_3\right)$, of multi-phase materials with uniaxial orientation [8]. No model is required to compute the CDF. Apart from fibre symmetry we only assume that the nanostructure is sufficiently imperfect. The CDF is the extension of Ruland's interface distribution function (IDF) [14] to the multidimensional case or, in a different view, the Laplacian of Vonk's multidimensional correlation function [15]. In the CDF peaks show up, where ever the displacement of the nanostructure with respect to itself generates areas of domain surface contact.

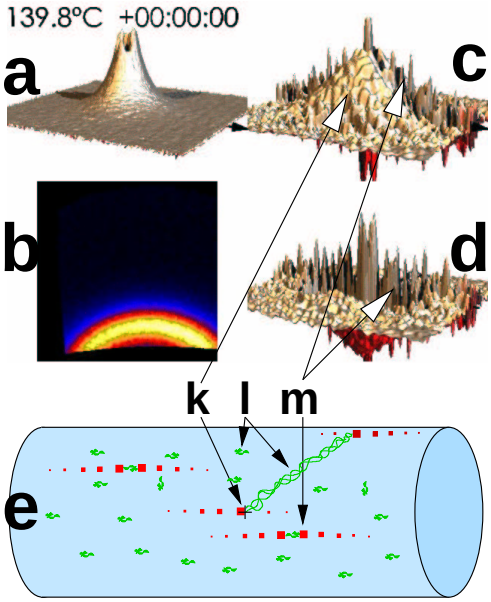

Figure 1: Structure of the oriented polyethylene melt. (a-d): Four views of the measured data are combined in one movie frame. (a): SAXS, (b): WAXS, (c): CDF (top view), (d) CDF (bottom view). Fibre axis in (b) vertical, otherwise horizontal. (e): Sketch of the nanostructure

3 Results and Discussion

The movies that show the nanostructure evolution in real space are available for download on the web (http://www.chemie.uni-hamburg.de/tmc/stribeck/crys/).

Figure 1 shows one movie frame from the beginning of the crystallisation containing combined measurement data (Figure 1a-d) and a sketch of the corresponding nanostructure (Figure 1e). The CDFs (c,d) display the correlations among domain surfaces in the nanostructure for displacements of 300 nm in two directions (fibre direction r_3 and transverse direction r_{12}, respectively). Fibre direction is indicated by an arrow in the base plane of the three-dimensional (3D) plots.

In the cooling melt we do not only observe the becoming and passing of crystal nuclei which form row structures along the fibre axis [16] (Figure 1, m). In addition, a broad pyramid-shaped elevation (Figure 1, k) shows up in the CDF which characterises correlations between opposite surfaces of some domains of irregular shape. The movies suggest that these domains are associated to the observed row nuclei. Thus we call them row nuclei associated domains (RADs). Moreover, the process of structure evolution indicates that the RADs may be identified by strands in the polymer chain network, in which chain entanglements are accumulated (Figure 1, l), the nuclei being located at the tips of these domains. By strands of different length and orientation this structure is governing a considerable but finite volume in the neighbourhood of a deliberate nucleus (Figure 1,k). This volume is confined by the extension of the pyramid shaped structure in the CDF. In the sketch (Figure 1e) it is indicated by the cylindrical envelope.

Upon increasing temperature of the melt we observe, how the material is loosing its memory [17]: The volume controlled by the RADs is shrinking, and when finally the correlations of the nuclei with each other are no longer restricted to the fibre direction, the material has lost most of its orientation memory.

Let us study a melt, the orientation memory of which is still fairly well preserved. Upon decreasing temperature the monotonous distribution between the tips of the RADs is developing maxima which move outward in correlation space (Figure 2, n). We interpret this phenomenon as a phase separation process causing the merging of entanglements into RADs. The maxima are not found on the meridian (fibre axis). Thus the most probable RAD is becoming an entangled strand that

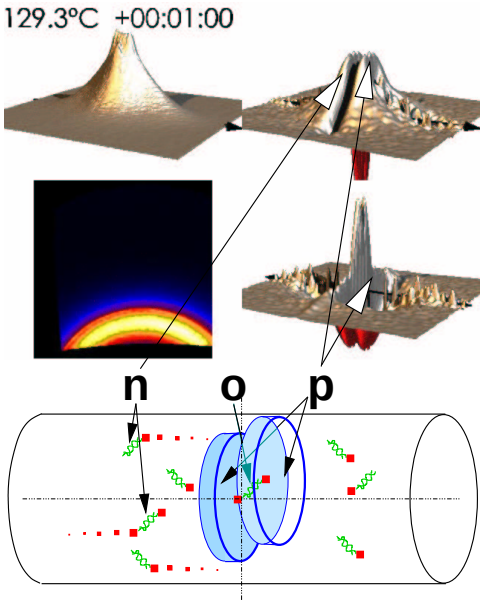

Figure 2: Primary lamellae have formed

is extending in an inclined direction.

Let us further restrict our demonstration to the case of isothermal crystallisation at 130°C (highest crystallisation temperature chosen). In this case the different mechanisms are most clearly separated from each other. In the beginning of crystallisation in the top view of the CDF (Figure 2, p) peaks from the first crystallites are showing up on the meridian, exactly between two RAD peaks. Thus their average thickness is more or less equal to the average extension of the RADs in fibre direction (24 nm). Their lateral extension cannot be read from the extension of the central peak, because it is veiled by the strong RAD peaks. Nevertheless, in the bottom view of the CDF we observe on the equator an extended self correlation triangle that is a typical feature of lamellar systems [8]. Continuous growth of the base of this triangle exhibits that most of the lamellae are continuously growing. Only a weak component from blocks arranged in planes [2] may be present.

Although the SAXS exhibits a high orientation, the orientation showing up in the WAXS pattern (pseudo colour image in Figure 2) is low.

The off-meridional RAD peaks do not vanish as crystallisation is proceeding. Instead, they are compressed in fibre direction and converted into offset layer thickness peaks describing amorphous gaps between neighbouring lamellae. A similar but reverse process is observed during the melting of the original material. Thus crystallisation appears to be governed by a peculiar nanostructure which we associate to the network [1, 18] of the entangled chains in the melt.

Based on these findings we propose a mechanism for the primary crystallisation. According to it, the extension of the most probable RADs in fibre direction and the lateral shift of their tips controls the primary lamellar structure. If an RAD is fertile at *both* ends (Figure 2, o), then its tips become the centres of two surfaces of offset neighbouring lamellae that are facing each other. In between is the amorphous layer with the entanglement-rich RAD. The inclination of the entangled strands that join two neighboured lamellae implies a component of lateral orientation of the corresponding amorphous region, as has been postulated by one of us in a model of crystallisation from a melt that is containing multi-functional knots of entangled strands of chain molecules [18].

In the following 20 min we observe that both meridional peaks visible in the top view of the CDF (Figure 3, black arrows) are moving in outward direction. Thus the average thickness of the crystalline layers is growing, but the distance between twin lamellae is kept constant. Thickness growth is oriented: away from the entanglement-rich RAD. During this phase the observed orientation of the

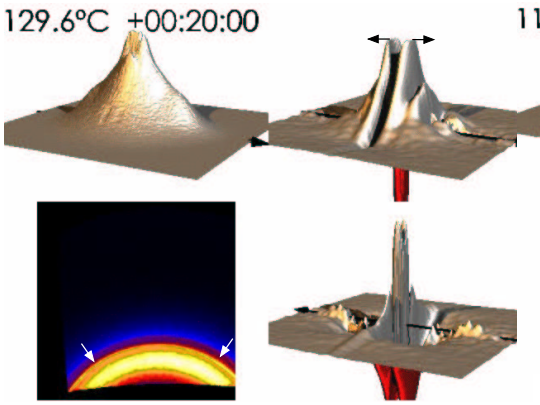

Figure 3: Thickness growth (black arrows) of lamellae has finished. Maximum orientation (white arrows) in the WAXS

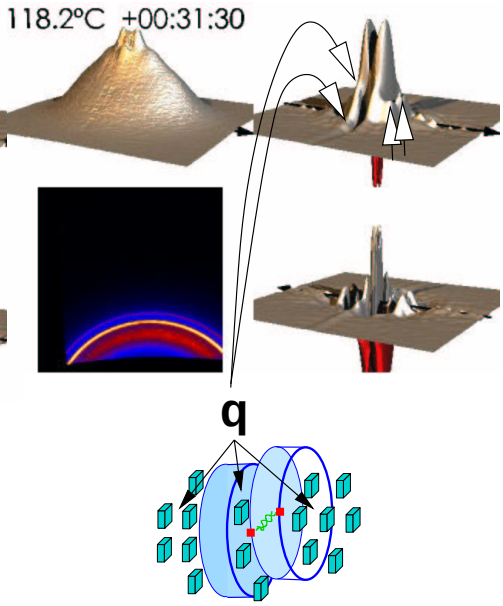

Figure 4: Swarms of block-shaped secondary crystals are formed (q). The WAXS becomes isotropic

WAXS reflections is increasing, as is the number of lamellae during this phase. After about 20 min this peculiar and more or less statistical placement process [10–12] of lamellae comes to an end.

In the final stage of crystallisation (Figure 4) the broad triangular peaks in the top view of the CDF are split into a series of narrow peaks, the strength of which is strongly decreasing as a function of distance from the meridian. This CDF feature is expected for an ensemble of separated blocks that are placed in a plane (Strobl [2]). Even a little bit earlier and on the meridian, strong but narrow correlation peaks start to grow, showing that along fibre direction the emerging blocks placed in such a way that they correlate strongly with each other. Anisotropy of the WAXS is lost during this phase, exhibiting that the blocky secondary crystals are not oriented.

In principle, our material passes through these phases even if the temperature profile is varied, but composition and size distributions of lamellae and blocks vary considerably. For example a narrow size distribution of secondary crystals (blocks) can be achieved by quenching from a high crystallisation temperature. Nevertheless, in all our experiments carried out under ambient pressure the ultimate nanostructure is governed by the short-ranging networks of frustrated crystal blocks.

4 Conclusions

Our in-situ melting and crystallisation experiments clearly show the evolution of the ensemble of crystalline domains and of the correlations among them. The method developed by us appears apt to elucidate the nanostructure evolution during processing and service of oriented polymer materials, in general. The only pre-requisition is that the process to be

investigated can be carried out at a synchrotron beam line equipped with modern detectors and in-situ control of the exposure. After the evaluation software is adapted to the actual setup, the complete processing beginning from the recorded scattering pattern up to the combined 3D view of the nanostructure is carried out automatically. Nevertheless, we are still far from a real-time visualisation of structure on a time-scale of seconds, which would require an increase of computing power by two orders of magnitude.

Acknowledgements. We thank the European Synchrotron Radiation Facility, Grenoble, for beam time granted in the frame of project SC 1396.

References

[1] Heck B, Hugel T, Iijima M, Sadiku E, Strobl G. New J Phys 1999; 1:17.1–17.29.

[2] Heck B, Hugel T, Iijima M, Strobl G. Polymer 2000;41(25):8839–8848.

[3] Heeley EL, Maidens AV, Olmsted PD, Bras W, Dolbnya IP, Fairclough JPA, Terrill NJ, Ryan AJ. Macromolecules 2003;36(10):3656–3665.

[4] Bras W, Dolbnya I, Detollenaere D, van Tol R, Malfois M, Greaves G, Ryan A, Heeley E. J Appl Cryst 2003;36(3):791–794.

[5] Somani RH, Yang L, Hsiao BH, Fruitwala H. J Macromol Sci Part B Phys 2003;B42(3):515–531.

[6] Somani RH, Yang L, Hsiao BS, Agarwal PK, Fruitwala HA, Tsou AH. Macromolecules 2002; 35(24):9096–9104.

[7] Yamazaki S, Hikosaka M, Toda A, Wataoka I, Yamada K, Tagashira K. J Macromol Sci Part B Physics 2003;B42(3-4):499–514.

[8] Stribeck N. J Appl Cryst 2001; 34(4):496–503.

[9] Stribeck N, Bayer R, von Krosigk G, Gehrke R. Polymer 2002; 43(13):3779–3784.

[10] Stribeck N, Almendarez Camarillo A, Cunis S, Bayer RK, Gehrke R. Macromol Chem Phys 2004; 205(11):1445–1454.

[11] Stribeck N. Macromol Chem Phys 2004;205(11):1455–1462.

[12] Stribeck N, Almendarez Camarillo A, Bayer R. Macromol Chem Phys 2004;205(11):1463–1470.

[13] pv-wave version 7.5. Pv–wave Version 7.5 (2001), Visual Numerics Inc., Boulder, Colorado.

[14] Ruland W. Colloid Polym Sci 1977; 255(5):417–427.

[15] Vonk CG. Colloid Polym Sci 1979; 257:1021–1032.

[16] Keller A, Machin MJ. J Macromol Sci Phys 1967;B1(1):41–91.

[17] Khanna YP, Kumar R, Reimschuessel AC. Polym Eng Sci 1988; 28(24):1607–1611.

[18] Bayer RK. Colloid Polym Sci 1994; 272(8):910–932.